Reforestation and crop land conversion impacts on future regional air quality in the Southeastern U.S.

M. Trail[1*], A.P. Tsimpidi[1], P. Liu[1], K. Tsigaridis[2, 3], Y. Hu[1], A. Nenes[4, 5], B. Stone[6], and A.G Russell[1]

[1]School of Civil & Environmental Engineering, Georgia Institute of Technology, Atlanta, GA 30332, USA

[2]Columbia Univ, Ctr Climate Syst Res, New York, NY USA

[3] NASA, Goddard Inst Space Studies, New York, NY 10025 USA

[4] School of Earth & Atmospheric Sciences, Georgia Institute of Technology, Atlanta, GA 30332, USA

[5]School of Chemical and Biomolecular Engineering, Georgia Inst. Technology, Atlanta, GA 30332, USA

[6]School of City and Regional Planning, Georgia Inst. Technology, Atlanta, GA 30332, USA

*Corresponding Author. Tel.:770 330 4601; E-mail address: mcus2rail@gmail.com

Abstract

Land in the southeastern U.S. is expected to change, e.g., given the potential demand to develop forest-to-fuel technologies or, conversely, cropification of current forests to increase food production. Possible future $PM_{2.5}$ and O_3 air quality for two land use/land cover change (LULCC) scenarios, reforestation and cropland conversion, are compared to a reference case scenario for the year 2050 using the Weather Research and Forecasting (WRF) and Community Multi-scale Air Quality (CMAQ) models. Changes in air quality driven by changes in climate, deposition and emissions relating to the LULCC are investigated.

Reforestation in the Southeast tends to decrease the ambient O_3 mixing ratio while slightly increasing summertime $PM_{2.5}$ in the Southeastern U.S. Results of a climate and deposition (CD) sensitivity simulation are provided for the two alternative LULCC scenarios to isolate the impact of changing climate and deposition on $PM_{2.5}$ and O_3 air quality. The sensitivity results indicate that deposition and emissions changes associated with reforestation impact O_3 and $PM_{2.5}$ concentrations as much as, and in most cases more than, changes in meteorology. Conversion of forest to cropland in the Southeast, on the other hand, tends to increase O_3 and increase $PM_{2.5}$ year-round. Cropland conversion leads to increased NO_X emissions and increases in the 4^{th} highest maximum daily 8-hr O_3 (MDA8) of the year by up to 10 ppb despite the tendency for increased deposition and decreased temperature to reduce the MDA8 mixing ratio. The results of this study show that O_3 and aerosol concentrations are sensitive to reforestation and cropland conversion in the Southeast and these land use changes should be considered in air quality management plans. Further, they show the sensitivity of such calculations to land cover properties.

Keywords LULCC, Climate Change, Air Quality, Reforestation

1 Introduction

Land use and land cover changes (LULCC) affect climate and air pollution. The southeastern U.S. underwent intense land use and land cover changes beginning in the 1700's [*Pacala et al.*, 2001; *Prestemon and Abt*, 2002; *Wear and Greis*, 2002; *Chen et al.*, 2006; *Steyaert and Knox*, 2008] and changes are expected to continue. In the 1700's forest land was converted to crops. More recently, cropland is being converted back to forest. Demand may grow to further develop forest-to-fuel technologies and increased use of wood products.

Conversely, there is also a demand for increased cropland. Physical parameters of certain crops and forests such as albedo, stomatal resistance and surface roughness affect climate by altering the land-atmosphere energy transfer [*Pielke et al.*, 1998] while land cover changes also effect the deposition of O_3 and $PM_{2.5}$ by altering the surface area and roughness for dry deposition of pollutants [*Pleim, J. E., Xiu, A., Finkelstein, P. L., and Otte*, 2002]. Changes in stomatal activity also effect the deposition of O_3 and other gases. Various vegetative species also emit volatile organic compounds (VOCs), precursors for ozone and secondary organic aerosol (SOA), and nitrogen oxides (NO_X), which is a precursor for ozone, at different rates [*Houweling et al.*, 1998; *Wang et al.*, 1998; *Racherla and Adams*, 2006; *Henze et al.*, 2007; *Liao et al.*, 2007].

Currently, there are 214 million acres of forested land in the South which only constitutes 60% of the forested land that existed in 1630 despite significant reforestation due to the growth of the timber industry since 1930 [*Wear and Greis*, 2002]. Around 60% of the nation's timber products are produced in the Southeast [*Prestemon and Abt*, 2002], and pine plantations have increased in the past few decades (from 2 million acres in 1953 to more than 30 million acres in 1999) [*Conner, R. C.*, 2002]. The growing demand to increase wood products-related industries and to develop forest-to-fuel technologies and bio-fuels from crops will continue to alter the land cover, and therefore the climate and air quality, in the Southeast. The impact that LULCC associated with bio-energy demand will have on future air quality is not well understood.

Although few studies have focused on investigating the impact of vegetative LULCC on air quality in the Southeastern U.S., recent studies have addressed LULCC on a regional scale in other regions [*Jiang et al.*, 2008] and on a global scale [*Ganzeveld*, 2004; *Wu et al.*, 2012]. Wu et al. [2012] found that potential global land cover changes caused by warmer climate and increased CO_2 abundance could lead to a general decrease in summertime

afternoon O_3 by up to 10 ppb. They report that the O_3 decreases are driven by increased O_3 dry deposition associated with increased vegetation density. In polluted regions, such as the northeastern U.S., however, O_3 and SOA increased due to higher isoprene emissions. Ganzeveld and Lelieveld [2004] found that deforestation in the Amazon Basin could decrease global isoprene emissions and O_3 deposition. Jiang et al. [2008] use the Weather Research Forecasting model with Chemistry (WRF/CHEM) to compare current and future air quality changes associated with climate change and land use change. They report that changing climate and urban land use can increase the daily maximum 8-hr O_3 mixing ratio by up to 6.2 ppb.

In this study, we use the Community Multi-scale Air Quality (CMAQ) model to compare possible future $PM_{2.5}$ and O_3 air quality for two LULCC scenarios to a reference case scenario for the year 2050. We investigate changes in air quality driven by changes in climate, deposition and emissions relating to the LULCC. We also provide results to climate and deposition (CD) sensitivity simulations for the two alternative LULCC scenarios to isolate the impact of changing climate and deposition on $PM_{2.5}$ and O_3 air quality. Inputs to CMAQ were prepared for a reforestation scenario, a cropland conversion scenario, and the current land cover (reference) scenario and include the regionally downscaled future climate results by the Weather Research Forecasting (WRF) model [*Trail et al.*, 2013a, 2013b] and emissions processed using the Sparse Matrix Operator Kernel Emissions (SMOKE) model. Energy related anthropogenic emissions inventories are projected to the future year levels using EPA US MARKAL 9r [*Rudokas et al.*, 2015]. The present study expands upon previous work [*Trail et al.*, 2014a, 2014b] in which we used the emissions inventories projected by MARKAL 9R to investigate the impact of various climate change mitigation strategies on U.S. air quality.

2 Methods

2.1 Meteorology

We use the non-hydrostatic Weather Research and Forecasting (WRF) Model [*Skamarock and Klemp*, 2008] (version 3.4) to downscale global climate to the regional scale. Initial and boundary conditions to the WRF are derived from meteorology simulated by the Goddard Institute for Space Studies (GISS) ModelE2 [*Schmidt et al.*, 2014]. Global simulations were carried out for the years 2006-2010 and 2048-2052 with a 3 year spin-up time and instantaneous outputs of physical parameters were produced at 6-hr intervals for regional downscaling by WRF. Simulations were driven by future atmospheric conditions over the 21st century and follow the scenario development process for IPCC AR5. The "Representative Concentration Pathway" (RCP) 4.5 [*Vuuren et al.*, 2011], where anthropogenic radiative forcing is 4.5 W m^{-2} in the year 2100 [*Moss et al.*, 2010], is used for this study. The global model domain has a horizontal resolution of 2°×2.5° latitude by longitude. The 40 layers of the global simulation follow a sigma coordinate up to 150 hPa, with constant pressure layers between 150 and 0.1 hPa.

Trail et al. [2013a], simulated regional climate for the years 2006-2010 and 2048-2052 with 10 day spin-up times, and the present study uses the meteorological results from the year 2050 which was found to be representative of that period. The model domain covers the contiguous United States (CONUS) and portions of southern Canada and northern Mexico with dimensions of 5328×4032 km and a grid-size of 36 km centered at 40°N and 97°W. The model domain contains 35 vertical levels, with the top pressure of 50hPa. The model scheme uses the Rapid Radiative Transfer Model (RRTM) [*Mlawer et al.*, 1997] and Dudhia scheme [*Dudhia*, 1989] for longwave and shortwave radiation respectively, the Yonsei University (YSU) [*Hong et al.*, 2006] scheme for the planetary boundary layer, the Noah scheme [*Ek*,

2003] for the land surface model (LSM), a revised version of Kain-Fritsch scheme [*Kain and Frisch*, 1993] to represent the effects of both deep and shallow cumulus clouds, and Lin scheme for modeling cloud microphysics [*Lin et al.*, 1983]. Spectral nudging of global model results is applied with a wave number of 2 in both zonal and meridional directions at 6 hour intervals [*Liu et al.*, 2012]. Spectral nudging is applied to horizontal winds at all vertical levels while temperature and geopotential heights are only nudged at layers above the planetary boundary layer (PBL). Trail et al. [2013a] evaluated the ability of GISS-WRF to reproduce the long-term yearly climatic means and the meteorological fields using 2006-2010 simulation and observations. Overall, the model performed well at simulating windspeed year-round (mean bias -0.1 to 0.2 m s^{-1}) and 2m temperatures during the spring, summer and fall (mean bias -2.7, -1.9 and 2.9 K, respectively). Wintertime simulated 2m temperature is biased low during for the entire U.S. (mean bias -7.5 K) but performs the best in the Southern U.S. (mean bias -4.5 K).

WRF simulations use the USGS 24-category landuse dataset. In this dataset, evergreen needleleaf forest, dryland cropland and pasture, deciduous broadleaf forest, and mixtures of these are the primary land cover categories in the Southeast U.S. In this study, we use the meteorology from the base scenario described in Trail et al. [2013b] and two southeastern LULCC scenarios. The reforestation scenario uses the meteorology simulated by converting all types of current cropland to evergreen needleleaf ("SE_for"), and the cropland conversion scenario uses meteorology simulated by converting all types of forest or forest mixture to dryland cropland and pasture ("SE_crop"). In the present study, the reforestation scenario most resembles the land use used in development of the RCP4.5 scenario, where cropland is reduced in the Southeastern U.S. by around 50% of the current crop area by 2100 and is mostly reforested. The cropland conversion scenario resembles the other RCP scenarios (2.6, 6.0 and 8.5) where cropland cover increases in the Southeast, with the RCP6.0 scenario

having the largest increase [*Vuuren et al.*, 2011; *Lawrence et al.*, 2012]. Loblolly and slash pine make up the majority of the pine species in the Southeast, though the USGS-24 category database does not differentiate between the species. Also, most of the cropland in the Southeast is made up of crops that are irrigated with overhead sprinklers, or semi-irrigated crops which are included in the dryland cropland category of the USGS dataset. The base case meteorology, (SE_norm) from Trail et al. [2013b], is used for the reference case. Surface air temperature increases between 1 and 2 °C in the base case meteorology compared to the present day meteorology (2010) over the Southeast during summer and fall. During the winter, surface temperature decreases by up to 1 °C [*Trail et al.*, 2013a].

Trail et al. [2013b] found that reforestation of crop regions in the Southeast with pine forest tends to lead to warming primarily due to the increase of stomatal resistance and decrease in albedo while the surface roughness increase may lessen the degree of warming by shifting the transfer of energy to the atmosphere from sensible to latent heat. Our results suggest that cooling tends to occur when forest is replaced with crop in the Southeast; though not enough to counter the simulated warming of 1-3 °C from greenhouse gas increases[*Trail et al.*, 2013b]. Cooling during the winter is attributed to the high albedo of cropland while during the spring and summer the decrease in stomatal resistance also contributes to cooling. Also increased LAI helps cool where deciduous forests are replaced with cropland.

2.2 Emissions

The Sparse Matrix Operator Kernel Emissions (SMOKE V3) model [*CEP*, 2003] produces hourly, gridded and speciated emissions for input to CMAQ. SMOKE uses inputs of the 2005 National Emissions Inventory (NEI) and ancillary data. To project emissions to 2050 levels, energy related emissions projection factors are calculated using the EPA MARKAL 9r model for the year 2050 [*Fishbone and Abilock*, 1981; *EPA*, 2006; *Loughlin et al.*, 2011;

176 *Rudokas et al.*, 2015]. MARKAL 9R models the energy system of the nine Census Divisions
177 of the U.S. and estimates future energy dynamics. Implementation of the following policies
178 were assumed in calculating the future emissions projections in MARKAL 9R: Clean Air Act
179 Title IV (Acid Rain Program) SO_2 and NO_X requirements, Clean Air Interstate Rule (CAIR),
180 Utility Mercury and Air Toxics Standards (MATS), Aggregated state Renewable Portfolio
181 (RPS) standards by region, Federal Corporate Average Fuel Economy (CAFE) standards as
182 modeled in AEO 2012, Tier 2 light duty vehicle tailpipe emission standards and heavy duty
183 vehicle fuel and engine rules. Non-energy related emissions were projected to 2050
184 according to the International Panel for Climate Change (IPCC) A1B scenario [*Woo et al.*,
185 2008]. Trail et al. [2014a] provide a summary of changes in future anthropogenic emission
186 rates and a sensitivity assessment of their impacts on air quality. Hourly emissions from U.S.
187 vegetation are computed using the Biogenic Emissions Inventory System (BEIS) and the
188 Biogenic Emissions Landcover Database 3.0 (BELD3). The resulting inventory consists of
189 pollutants emitted from area, mobile, point, fire, ocean, biogenic, and agricultural sources.
190 The BELD3 database consists of 229 categories, including 17 crop types, 193 species of tree
191 and 19 USGS categories. For every grid cell in the domain, the fraction of each vegetation
192 category is specified. The primary tree species in the Southeast are loblolly and jack pine
193 while crops in the Southeast are more varied by region and include tobacco, wheat, cotton,
194 corn, soybean and others. Each vegetation type has corresponding emission factors for 34
195 chemical species including isoprene, carbon monoxide and nitrous oxide (Table 1). In
196 developing the biogenic emissions for the reforestation scenario, all crops in the Southeast
197 domain were converted to loblolly pine since loblolly pine is commonly used in the timber
198 industry (Figure 1a). Biogenic emissions for the cropland conversion scenario were
199 developed by converting all tree species to the most common crop within a particular grid cell
200 (Figures 1b). For example, if 60% of the land in a grid cell is covered by tree species, 20% is

urban, 15% is corn and 5% is cotton, then the 60% of land covered by trees will be changed to corn. In this scenario, tree species are primarily converted to corn with some land being converted to cotton (Figures 1b and c) roughly in proportion to current crops. Biogenic emissions changes in this study do not include altered emissions from wildfires and prescribed burns related to reforestation and cropland conversion. Also, the potential for isoprene emission inhibition by rising CO_2 concentrations [*Young et al.*, 2008; *Tai et al.*, 2013] is not included in these simulations.

2.3 Air Quality

We use the CMAQ 4.7.1 [*Foley et al.*, 2010] to simulate the transformation and fate of air pollutants for the future (2050) reference case and for the two LULCC scenarios. A spin-up period of 10 days for each simulation minimizes the influence of the initial conditions. Gas-phase chemistry is modeled using the SAPRC-99 [*Carter*, 1999] chemical mechanism. The domain covers the entire contiguous U.S. as well as portions of Canada and Mexico (5328×4032 km). The modeling domain uses a Lambert Conformal Projection with true latitudes of 33ºN and 45ºN centered at 40ºN, 97ºW. A horizontal grid with a 36x36-km resolution is used with thirteen vertical layers extending ~15.9 km above ground. There are 7 layers below 1 km and the first layer is 18 m thick. Future dynamic boundary conditions are taken from the GISS global simulation while the default CMAQ initial conditions of pollutant concentrations are used. Dry deposition velocities are calculated using an electrical resistance analog model where the canopy resistance is a parallel combination of surface resistances and stomatal resistance [*Pleim, J. E., Xiu, A., Finkelstein, P. L., and Otte*, 2002; *Otte and Pleim*, 2009]. Dry deposition is calculated using parameters from the USGS 24-category database. The stomatal resistance value for the USGS "evergreen needleleaf" category is used for

loblolly pine in this study [*UCAR*, 2008]. Similarly, the "dryland/cropland and pasture" stomatal resistance is used for all cropland conversion species.

In addition to the two LULCC scenarios, which span the entire year 2050, a climate and deposition (CD) sensitivity case is simulated for a winter (Jan) and a summer (Jul) month to isolate the effects of altered climate and deposition associated with LULCC on ambient air pollutant concentrations. For the CD scenarios, we fix the biogenic emissions for each scenario to the reference case emissions while using the meteorology and deposition from the two LULCC scenarios.

Trail et al. [2014a] provide a detailed description and evaluation of the CMAQ model set up. The CMAQ simulations were evaluated by simulating air quality over the U.S. for the year 2010 using downscaled 2010 global climate and emissions projected to the year 2010 and comparing the results to Environmental Protection Agency (EPA) Air Quality System (AQS) data. Trail et al. [2014a] found that simulated surface $PM_{2.5}$ and O_3 show good agreement with observations for the year 2010. Simulated 2010 MDA8 O_3 was biased high, however, the cumulative distribution of the MDA8 results agree best with observations at higher MDA8 O_3 concentration in most regions. The annual mean $PM_{2.5}$ was biased low (normalized mean bias of -21%) with the largest negative bias occurring during the summer. The study also highlights notable changes in U.S. air quality from 2010 to 2050. In particular reductions in anthropogenic NO_X emissions result in increased sensitivity of O_3 to NO_X emissions over almost all of the domain, including in the Southeast. The study also showed reduced sensitivity of O_3 to VOC emissions. However, reduced VOC emissions resulting from the inclusion of CO_2 inhibition of isoprene emissions could reduce the magnitude of the resulting changes in O_3 sensitivity to VOC and NO_X.

3 Results

3.1 Reforestation

Trail et al. [2014a] compared present and future U.S. air quality and found overall decreases in O_3 and $PM_{2.5}$ during summer and small increases in $PM_{2.5}$ during winter. They compare the changed in the 4th highest mean daily 8-hr average (MDA8) O_3 mixing ratio of the year, which is the metric used to determine if an area is in non-attainment according to the National Ambient Air Quality Standard (NAAQS). The current NAAQS standard is 75 ppb. In the present study, reforestation leads to decreased 4th highest MDA8 of the year by up to 10 ppb from the reference case in the Southeastern U.S. (Figure 2). Decreased 4th highest MDA8 occurs mostly over Mississippi, Alabama, Tennessee, Arkansas, and southern Kentucky while Georgia and the Carolinas experience small decreases. Reforestation of cropland leads to decreased emissions of NO_X and therefore decreased O_3 mixing ratio in NO_X limited environments (Table 1). However, land use changes also alter regional meteorology and deposition rates of pollutants.

The CD scenario isolates the impacts of changing meteorology and deposition from land use change to air quality by fixing the emissions to the reference case emissions for one month during the O_3 season. While isoprene emissions are a main mechanism through which meteorology affects ozone air quality, changes in isoprene emissions due to temperature changes are not captured in the CD scenario since emissions are fixed to the reference case. The summertime one-month average MDA8 decreases by up to 3 ppb in the CD scenario over the same regions where the largest decreases in 4th highest MDA8 occur near the Mississippi river (Figure 2). In this region, although some localized deposition decreases are seen where crop is replaced with pine, reforestation mostly leads to O_3 deposition increases where a cropland/woodland mixture is replaced with pine, leading to more efficient removal of O_3 from the atmosphere (Figure 2). Mixed crop/woodland is converted to pine in this region and

Trail et al. [2013b] predicted potential decreases in daytime temperature due to increased soil moisture and therefore increased evaporation, especially in Mississippi. Temperature decreases in this region also lead to lower MDA8 O_3 mixing ratio. Therefore, over Arkansas, Tennessee and Kentucky, decreases in the 4th highest MDA8 O_3 are caused by decreased emissions of NO_X, increased deposition from reforestation of crops/woodland areas and decreased daytime temperatures. Further, decreased temperature from reforestation leads to reduced ozone via reduced isoprene emissions, although this is not apparent from the CD scenario.

Over the Eastern regions of Georgia and the Carolinas on the other hand, summertime one-month average MDA8 increases by up to 3 ppb in the CD scenario. Deposition of O_3 decreases due to reforestation in Georgia and the Carolinas where pure crop is converted to pine, contributing to the increased MDA8 O_3 over those regions (Figure 2). Loblolly pine has a higher stomatal resistance than cropland, so the overall flux of trace gases into the leaf is reduced despite increased leaf area. Also, increased simulated temperatures over Georgia and the Carolinas enhance O_3 formation. In this region, lower NO_X emissions reduces O_3, though enhanced formation from warming and reduced removal efficiency from deposition changes tend to increase ambient levels of O_3.

Summertime (JJA) average $PM_{2.5}$ concentration increases of up to 1 μg m^{-3} occur over the Southeast due to reforestation of croplands with the largest increases over the Mississippi river and in Georgia and South Carolina (Figure 3a). Summertime average organic matter (OM) aerosol increases by 0.35 μg m^{-3}, averaged over the southeast region, while nitrate and sulfate aerosol concentrations experience small changes (Table 2). In the CD scenario however, $PM_{2.5}$ and OM concentrations decrease by around 1 μg m^{-3} and 0.47 μg m^{-3} (Figure 3b). Deposition of $PM_{2.5}$ increases in Georgia, South Carolina and southern Missouri, which would lead to decreased concentrations of $PM_{2.5}$ (Figure 3b), meaning that increased

emissions of organic compounds from reforestation lead to higher concentrations of $PM_{2.5}$ despite the tendency for meteorology and deposition changes to decrease $PM_{2.5}$ concentration. During the winter, there are small decreases in seasonal average $PM_{2.5}$ concentration of up to 0.5 $\mu g\ m^{-3}$ (Figure 4a). The CD scenario shows similar decreased PM concentrations (Figure 4b) while deposition increases slightly (Figure 4c). During wintertime, increased biogenic VOC emissions lead to higher concentrations of OM, while increased deposition leads to lower concentration of total $PM_{2.5}$. Also, regional warming from reforestation leads to decreased partitioning of volatile components of $PM_{2.5}$, like nitrate, to the particle phase, further reducing $PM_{2.5}$ concentration, though this effect is small.

3.2 Cropland Conversion

Conversion of forest to cropland in the Southeast leads to increases in 4th highest MDA8 mixing ratio in Mississippi, Alabama, Georgia, and South Carolina of up to 10 ppb (Figure 2a). Cropland emits NO_X at a much higher rate than forest due to microbial activity and fertilization, leading to this increased production of O_3 in the atmosphere. On the other hand, decreased 4th highest MDA8 occur in Louisiana, Arkansas, Tennessee, and South Missouri by up to 6 ppb even though NO_X emissions increase. Reduced O_3 here results from increased deposition as seen in the CD scenario, where the month average MDA8 also decreases over most of the Southeastern domain with the largest decreases (up to 7 ppb) occurring over Arkansas, Tennessee, and northern Mississippi (Figure 2b). Cooling would also reduce isoprene emissions in the region and thus reduce O_3, however as noted previously, this dependence is not simulated in the CD scenario. Increased O_3 deposition follows a similar spatial pattern as the decreased MDA8 for the CD scenario, indicating that increased deposition, resulting from reduced stomatal resistance, leads to decreased MDA8 O_3 mixing ratios in regions of crop land conversion (Figure 2c). Similar to the reforestation scenario,

changes in stomatal activity, when land cover is converted from forest to crop, affect deposition rates of trace gases more than changes in leaf area index. Further, decreased temperatures due to cropland conversion reduce O_3 production.

Seasonal average $PM_{2.5}$ concentration over the Southeast domain increases by up to 1.5 μg m^{-3} in the cropland conversion scenario occur during winter and summer (Figures 3a and 4a). During the summer, sulfate aerosol average over the Southeast domain increases by 0.67 μg m^{-3} while OM aerosol decreases by 0.41 μg m-3 (Table 2). The decreased OM results from lower emissions of organic compounds, such as isoprene, from crops rather than from forests while increased sulfate results from reduced deposition (Table 2). Increased $PM_{2.5}$ concentration of up to 1 μg m^{-3} also occurs in the CD scenario during winter and summer (Figures 3b and 4b). Aerosol deposition decreases during the summer, because the surface roughness is reduced where forest is converted to crop, contributing to increased aerosol concentrations (Figure 3c). During the winter decreased deposition and increased NO_X emission rates lead to increased nitrate aerosol concentration of 0.31 μg m^{-3} averaged over the Southeast domain (Table 2 and Figure 4).

4 Summary and Conclusions

We investigated the impacts of potential reforestation and cropland conversion on future regional air quality in the Southeastern U.S. using downscaled meteorology from a general circulation model and emissions projected to 2050. We explore how altered precursor biogenic emissions, deposition rates and meteorology associated with reforestation and cropland conversion influence ambient O_3 and $PM_{2.5}$ concentrations. Reforestation tends to decrease the 4^{th} highest MDA8 O_3 of the year while increasing summertime $PM_{2.5}$ in the Southeast. Conversion of forest to cropland, on the other hand, tends to increase the 4^{th}

highest MDA8 O_3 of the year and increase $PM_{2.5}$ year-round. Other studies [*Chen et al.*, 2009; *Wu et al.*, 2012; *Tai et al.*, 2013] simulate decreased O_3 resulting from cropland expansion in the U.S. and conclude that the O_3 decreases result from reduced VOC emissions in NO_X-rich air. The same studies used either present day emissions or future projections of emissions and some included CO_2 inhibition of isoprene emissions that lead to a more NO_X-rich environment. The present study, however, uses future emissions projections that lead to a more NO_X-limited environment over much of the Southeast except over major cities, in agreement with recent studies using both ground-based and satellite data [*Duncan et al.*, 2010; *Fisher et al.*, 2014; *Lei and Wang*, 2014]. However, rising CO_2 concentration in the future may inhibit isoprene emissions and therefore impact whether the environment remains NO_X-limited. The differences in cropland expansion impact on O_3 in the present study and previous studies highlight the import role that anthropogenic emissions play when considering land use change impacts on atmospheric chemistry.

In a previous study, Trail et al. [2013b] analyzed the meteorology used in the present study and predicted that changes in meteorology related to reforestation of cropland leads to warming and potentially enhanced production of O_3, except over the Mississippi river where cooling occurs. In the present study however, we find that deposition and emissions changes impact O_3 and $PM_{2.5}$ concentrations as much as, and in most cases more than, changes in meteorology. For example, where Trail et al. [2013b] predicted enhanced production of O_3 due to reforestation, we found little change in O_3 concentration because of decreased biogenic NO_X emissions.

Trail et al. [2013b] also note the importance in understanding the uncertainty associated with vegetation parameters when simulating the impact of agricultural changes on regional climate due to the regional climate sensitivity to parameters such as the stomatal resistance. In the present study, air pollution concentrations are sensitive to the parameters

used in calculating biogenic emissions and deposition, such as leaf area index and emission factors. The results of this study further the findings of studies aimed at understanding strategies to improve future air quality by showing that O_3 and aerosol concentrations are sensitive to reforestation and cropland conversion in the Southeast and such land use changes should be considered in air quality management plans. Further, this study isolates the impacts of LULCC-related climate change and deposition rates, and shows the sensitivities of such calculations to land cover properties.

5 Acknowledgments

While this work was supported, in part, by grants from the US EPA (RD-83428101) and NASA, reference herein to any specific commercial products, process, or service by trade name, trademark, manufacturer, or otherwise, does not necessarily constitute or imply their endorsement or recommendation. The views and opinions of authors expressed herein are those of the authors and do not necessarily state or reflect those of the United States Government.

6 References

Carter, W. P. L. (1999), Documentation of the SAPRC-99 Chemical Mechanism for VOC Reactivity Assessment, *Assessment*, *1*, 329.

CEP (2003), Sparse Matrix Operator Kernel Emissions Modeling System (SMOKE) User Manual,

Chen, H., H. Tian, M. Liu, J. Melillo, S. Pan, and C. Zhang (2006), Effect of land-cover change on terrestrial carbon dynamics in the southern United States., *J. Environ. Qual.*, *35*, 1533–47, doi:10.2134/jeq2005.0198.

Chen, J., J. Avise, A. Guenther, C. Wiedinmyer, E. Salathe, R. B. Jackson, and B. Lamb (2009), Future land use and land cover influences on regional biogenic emissions and air quality in the United States, *Atmos. Environ.*, *43*, 5771–5780, doi:10.1016/j.atmosenv.2009.08.015.

Conner, R. C., and A. J. H. (2002), *The Southern Forest Resource Assessment: Chapter 16, Forest Area and Conditions: Chapter 16, Forest Area and Conditions*, edited by S. R. S. Department of Agriculture, Forest Service.

Dudhia, J. (1989), Numerical Study of Convection Observed during the Winter Monsoon Experiment Using a Mesoscale Two-Dimensional Model, *J. Atmos. Sci.*, *46*, 3077–3107, doi:10.1175/1520-0469(1989)046<3077:NSOCOD>2.0.CO;2.

Duncan, B. N. et al. (2010), Application of OMI observations to a space-based indicator of NOx and VOC controls on surface ozone formation, *Atmos. Environ.*, *44*(18), 2213–2223, doi:10.1016/j.atmosenv.2010.03.010.

Ek, M. B. (2003), Implementation of Noah land surface model advances in the National Centers for Environmental Prediction operational mesoscale Eta model, *J. Geophys. Res.*, *108*, doi:10.1029/2002JD003296.

EPA (2006), EPA U. S. National MARKAL Database, *United States Environ. Prot. Agency*.

Fishbone, L. G., and H. Abilock (1981), Markal, a Linear-Programming Model for Energy-Systems Analysis - Technical Description of the Bnl Version, *Int. J. Energy Res.*, *5*, 353–375, doi:10.1002/er.4440050406.

Fisher, J. A., D. J. Jacob, P. S. Kim, K. R. Travis, L. Zhu, and K. Yu (2014), Using SEAC4RS observations to improve modeling of isoprene chemistry in GEOS-Chem, in *SEAC4RS Science Team Meeting, Poster*.

Foley, K. M. et al. (2010), Incremental testing of the Community Multiscale Air Quality (CMAQ) modeling system version 4.7, *Geosci. Model Dev.*, *3*, 205–226, doi:10.5194/gmd-3-205-2010.

Ganzeveld, L. (2004), Impact of Amazonian deforestation on atmospheric chemistry, *Geophys. Res. Lett.*, *31*, doi:10.1029/2003GL019205.

Henze, D. K., J. H. Seinfeld, N. L. Ng, J. H. Kroll, T.-M. Fu, D. J. Jacob, and C. L. Heald (2007), Global modeling of secondary organic aerosol formation from aromatic hydrocarbons: high- vs low-yield pathways, *Atmos. Chem. Phys. Discuss.*, *7*, 14569–14601, doi:10.5194/acpd-7-14569-2007.

Hong, S.-Y., Y. Noh, and J. Dudhia (2006), A New Vertical Diffusion Package with an Explicit Treatment of Entrainment Processes, *Mon. Weather Rev.*, *134*, 2318–2341, doi:10.1175/MWR3199.1.

Houweling, S., F. Dentener, and J. Lelieveld (1998), The impact of nonmethane hydrocarbon compounds on tropospheric photochemistry, *J. Geophys. Res.*, *103*, 10673, doi:10.1029/97JD03582.

Jiang, X. Y., C. Wiedinmyer, F. Chen, Z. L. Yang, and J. C. F. Lo (2008), Predicted impacts of climate and land use change on surface ozone in the Houston, Texas, area, *J. Geophys. Res.*, *113*, doi:D20312\r10.1029/2008jd009820.

Kain, J., and J. Frisch (1993), Convective parameterization for mesoscale models: The kain-fritsch scheme, *Meteorol. Monogrpahs*, *24*, 165–170.

Lawrence, P. J. et al. (2012), Simulating the biogeochemical and biogeophysical impacts of transient land cover change and wood harvest in the Community Climate System Model (CCSM4) from 1850 to 2100, *J. Clim.*, *25*, 3071–3095, doi:10.1175/JCLI-D-11-00256.1.

Lei, H., and J. X. L. Wang (2014), Sensitivities of NOx transformation and the effects on surface ozone and nitrate, *Atmos. Chem. Phys.*, *14*(3), 1385–1396, doi:10.5194/acp-14-1385-2014.

Liao, K. J., E. Tagaris, K. Manomaiphiboon, S. L. Napelenok, J. H. Woo, S. He, P. Amar, and A. G. Russell (2007), Sensitivities of ozone and fine particulate matter formation to emissions under the impact of potential future climate change, *Environ. Sci. Technol.*, *41*, 8355–8361, doi:10.1021/es070998z.

Lin, Y.-L., R. D. Farley, and H. D. Orville (1983), Bulk Parameterization of the Snow Field in a Cloud Model, *J. Clim. Appl. Meteorol.*, *22*, 1065–1092, doi:10.1175/1520-0450(1983)022<1065:BPOTSF>2.0.CO;2.

Liu, P., A. P. Tsimpidi, Y. Hu, B. Stone, A. G. Russell, and A. Nenes (2012), Differences between downscaling with spectral and grid nudging using WRF, *Atmos. Chem. Phys.*, *12*(8), 3601–3610, doi:10.5194/acp-12-3601-2012.

Loughlin, D. H., W. G. Benjey, and C. G. Nolte (2011), ESP v1.0: Methodology for exploring emission impacts of future scenarios in the United States, *Geosci. Model Dev.*, *4*, 287–297, doi:10.5194/gmd-4-287-2011.

Mlawer, E. J., S. J. Taubman, P. D. Brown, M. J. Iacono, and S. A. Clough (1997), Radiative transfer for inhomogeneous atmospheres: RRTM, a validated correlated-k model for the longwave, *J. Geophys. Res.*, *102*, 16663, doi:10.1029/97JD00237.

466 Moss, R. H. et al. (2010), The next generation of scenarios for climate change research and
467 assessment., *Nature*, *463*, 747–756, doi:10.1038/nature08823.

468 Otte, T. L., and J. E. Pleim (2009), The Meteorology-Chemistry Interface Processor (MCIP)
469 for the CMAQ modeling system, *Geosci. Model Dev. Discuss.*, *2*, 1449–1486,
470 doi:10.5194/gmdd-2-1449-2009.

471 Pacala, S. W. et al. (2001), Consistent land- and atmosphere-based U.S. carbon sink
472 estimates., *Science*, *292*, 2316–2320, doi:10.1126/science.1057320.

473 Pielke, R. A., R. Avissar, M. Raupach, A. J. Dolman, X. Zeng, and A. S. Denning (1998),
474 Interactions between the atmosphere and terrestrial ecosystems: influence on weather
475 and climate, *Glob. Chang. Biol.*, *4*, 461–475, doi:10.1046/j.1365-2486.1998.00176.x.

476 Pleim, J. E., Xiu, A., Finkelstein, P. L., and Otte, T. L. (2002), A coupled land-surface and
477 dry deposition model and comparison to field measurements of surface heat, moisture,
478 and ozone fluxes, *Water Air Soil Pollut.*, *1*, 243–252.

479 Prestemon, J. P., and R. C. Abt (2002), The southern timber market to 2040, *J. For.*, *100*, 16–
480 23.

481 Racherla, P. N., and P. J. Adams (2006), Sensitivity of global tropospheric ozone and fine
482 particulate matter concentrations to climate change, *J. Geophys. Res. Atmos.*, *111*,
483 doi:10.1029/2005JD006939.

484 Rudokas, J., P. Miller, M. Trail, and A. G. Russell (2015), Regional Air Quality Management
485 Aspects of Climate Change: Impact of Climate Mitigation Options on Regional Air
486 Emissions, *Environ. Sci. Technol.*

487 Schmidt, G. A. et al. (2014), Configuration and assessment of the GISS ModelE2
488 contributions to the CMIP5 archive, *J. Adv. Model. EARTH Syst.*, *6*(1), 141–184,
489 doi:10.1002/2013MS000265.

490 Skamarock, W. C., and J. B. Klemp (2008), A time-split nonhydrostatic atmospheric model
491 for weather research and forecasting applications, *J. Comput. Phys.*, *227*, 3465–3485,
492 doi:10.1016/j.jcp.2007.01.037.

493 Steyaert, L. T., and R. G. Knox (2008), Reconstructed historical land cover and biophysical
494 parameters for studies of land-atmosphere interactions within the eastern United States,
495 *J. Geophys. Res. Atmos.*, *113*, doi:10.1029/2006JD008277.

496 Tai, A. P. K., L. J. Mickley, C. L. Heald, and S. Wu (2013), Effect of CO2 inhibition on
497 biogenic isoprene emission: Implications for air quality under 2000 to 2050 changes in
498 climate, vegetation, and land use, *Geophys. Res. Lett.*, *40*(13), 3479–3483,
499 doi:10.1002/grl.50650.

500 Trail, M., A. P. Tsimpidi, P. Liu, K. Tsigaridis, Y. Hu, A. Nenes, and A. G. Russell (2013a),
501 Downscaling a global climate model to simulate climate change over the US and the
502 implication on regional and urban air quality, *Geosci. Model Dev.*, *6*(5), 1429–1445.

503 Trail, M., A. P. Tsimpidi, P. Liu, K. Tsigaridis, Y. Hu, A. Nenes, B. Stone, and A. G. Russell
504 (2013b), Potential impact of land use change on future regional climate in the
505 Southeastern U.S.: Reforestation and crop land conversion, *J. Geophys. Res. Atmos.*,
506 *118*(20), 11577–11588.

507 Trail, M., A. P. Tsimpidi, P. Liu, K. Tsigaridis, J. Rudokas, P. Miller, Y. Hu, A. Nenes, and
508 A. G. Russell (2014a), Impact of potential future carbon policies and climate change on
509 United States regional air quality, *Environ. Sci. Technol. Submitt.*

510 Trail, M., A. P. Tsimpidi, P. Liu, K. Tsigaridis, J. Rudokas, P. Miller, A. Nenes, Y. Hu, and
511 A. G. Russell (2014b), Sensitivity of air quality to potential future climate change and
512 emissions in the United States and major cities, *Atmos. Environ.*, *94*, 552–563,
513 doi:10.1016/j.atmosenv.2014.05.079.

514 UCAR (2008), Chapter 3: WRF Preprocessing System (WPS), Available from:
515 http://www2.mmm.ucar.edu/wrf/users/docs/user_guide_V3/users_guide_chap3.htm

516 Vuuren, D. P. et al. (2011), The representative concentration pathways: an overview, *Clim.*
517 *Change*, *109*(1-2), 5–31, doi:10.1007/s10584-011-0148-z.

518 Wang, Y., J. a Logan, and D. J. Jacob (1998), Global simulation of tropospheric O 3 -NO x -
519 hydrocarbon chemistry 2. Model evaluation and global ozone budget, *J. Geophys. Res.*,
520 *103*, 10727–10755, doi:10.1029/98JD00157.

521 Wear, D. N., and J. G. Greis (2002), Southern forest resource assessment: summary of
522 findings, *J. For.*, *100*, 6–14.

523 Woo, J.-H., S. He, E. Tagaris, K.-J. Liao, K. Manomaiphiboon, P. Amar, and A. G. Russell
524 (2008), Development of North American emission inventories for air quality modeling
525 under climate change., *J. Air Waste Manag. Assoc.*, *58*, 1483–1494, doi:10.3155/1047-
526 3289.58.11.1483.

527 Wu, S., L. J. Mickley, J. O. Kaplan, and D. J. Jacob (2012), Impacts of changes in land use
528 and land cover on atmospheric chemistry and air quality over the 21st century, *Atmos.*
529 *Chem. Phys.*, *12*, 1597–1609, doi:10.5194/acp-12-1597-2012.

530 Young, P. J., A. Arneth, G. Schurgers, G. Zeng, and J. A. Pyle (2008), The CO_2 inhibition of
531 terrestrial isoprene emission significantly affects future ozone projections, *Atmos. Chem.*
532 *Phys. Discuss.*, *8*, 19891–19916, doi:10.5194/acpd-8-19891-2008.

533
534

535

Table 1 Emission rates of Isoprene and NO for the vegetation categories that change the most in the LULCC scenarios.

	Isoprene ($gC/(km^2\ hr)$)	Nitrous Oxide ($gN/(km^2\ hr)$)
Loblolly Pine	70	2
Corn	1	68
Cotton	7	45

Table 2 Concentrations of major $PM_{2.5}$ species during the winter (DJF) and summer (JJA) and for the summertime CD scenarios (July) for the reference case and the change in concentrations for the two LULCC scenarios (scenario minus reference case). OM is organic matter, NO_3 is nitrate aerosol and SO_4 is sulfate aerosol.

	Reference case (ug m-3)			Reforestation change (ug m-3)			Cropland Conversion change (ug m-3)		
	Win	Sum	Sum CD	Win	Sum	Sum CD	Win	Sum	Sum CD
OM	1.14	1.16	0.96	0.37	0.35	-0.47	0.00	-0.41	0.01
NO3	1.12	0.03	0.04	-0.18	-0.01	0.00	0.31	0.11	0.01
SO4	1.30	1.90	1.90	0.07	0.06	-0.08	0.10	0.67	0.01

547 **(a)**

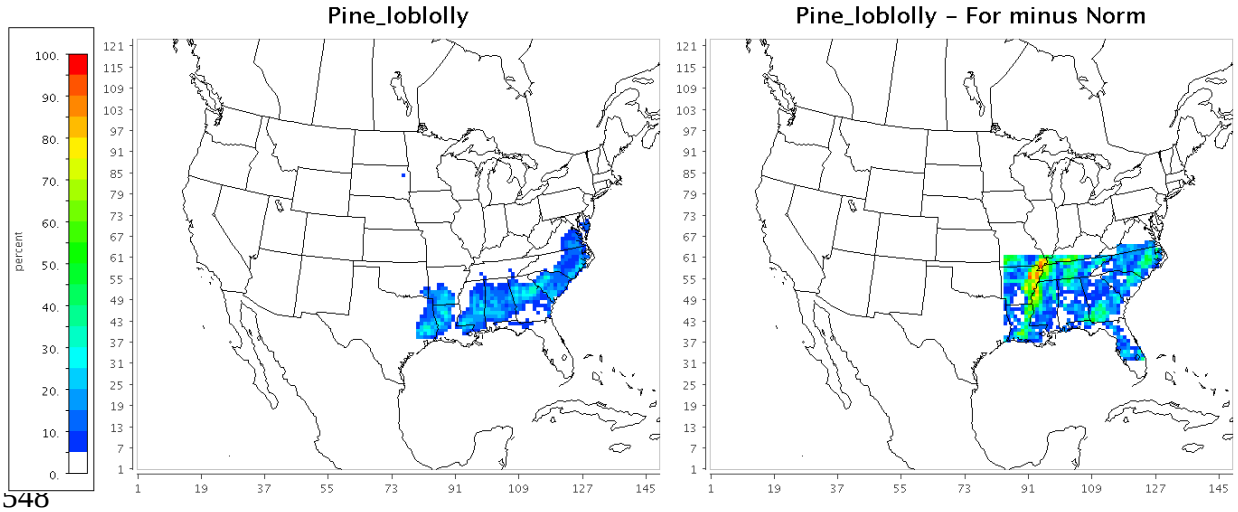

548

549 **(b)**

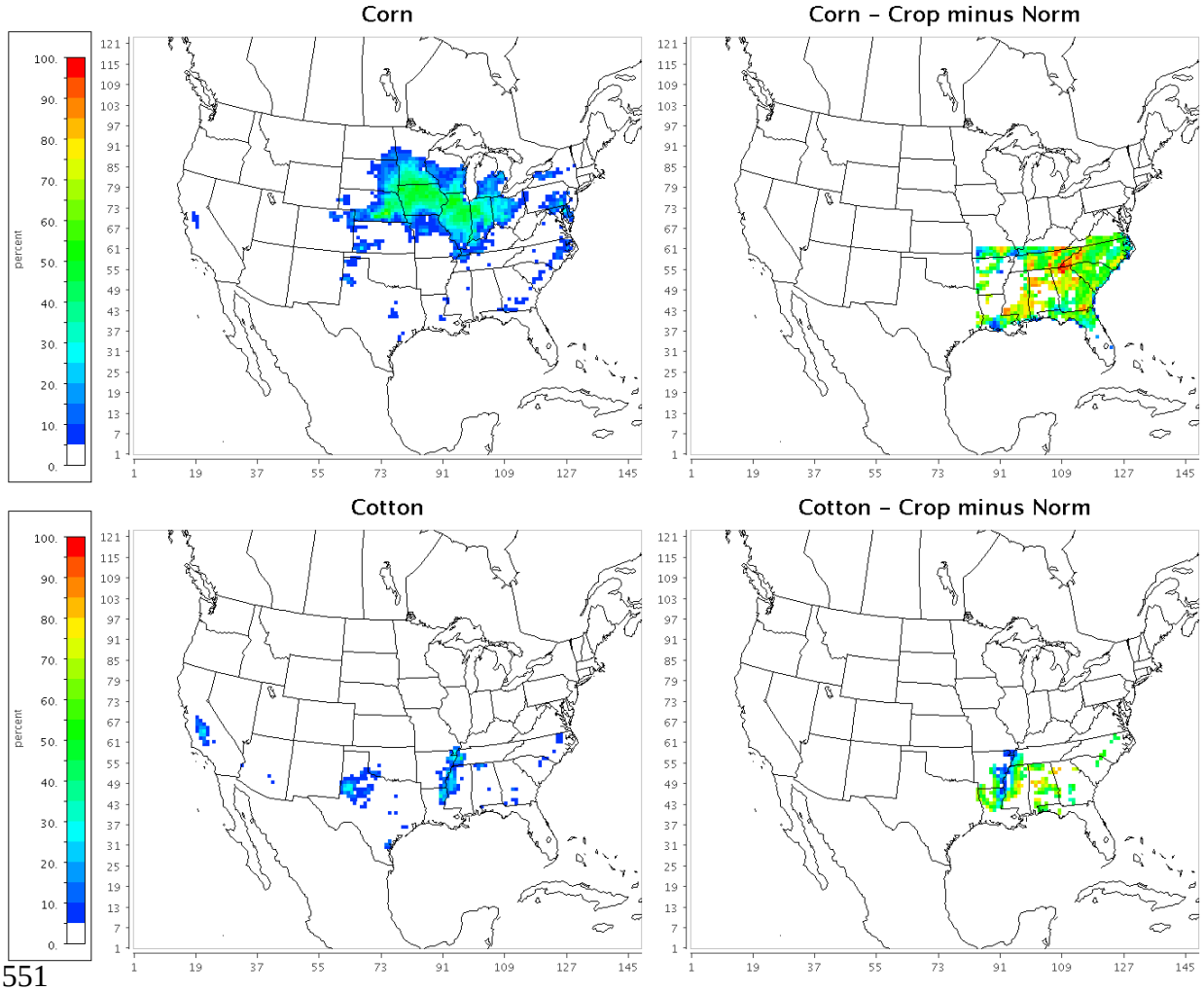

551

552 **Figure 1 (a)** Percentage of loblolly pine in the original BELD3 landuse dataset (left) and the
553 change in loblolly pine for the reforestation scenario (right). **(b)** Percentage of corn (top) and
554 cotton (bottom) crop in the original BELD3 dataset (left column) and the change in corn and
555 cotton crop for the cropland conversion scenario (right column).

556

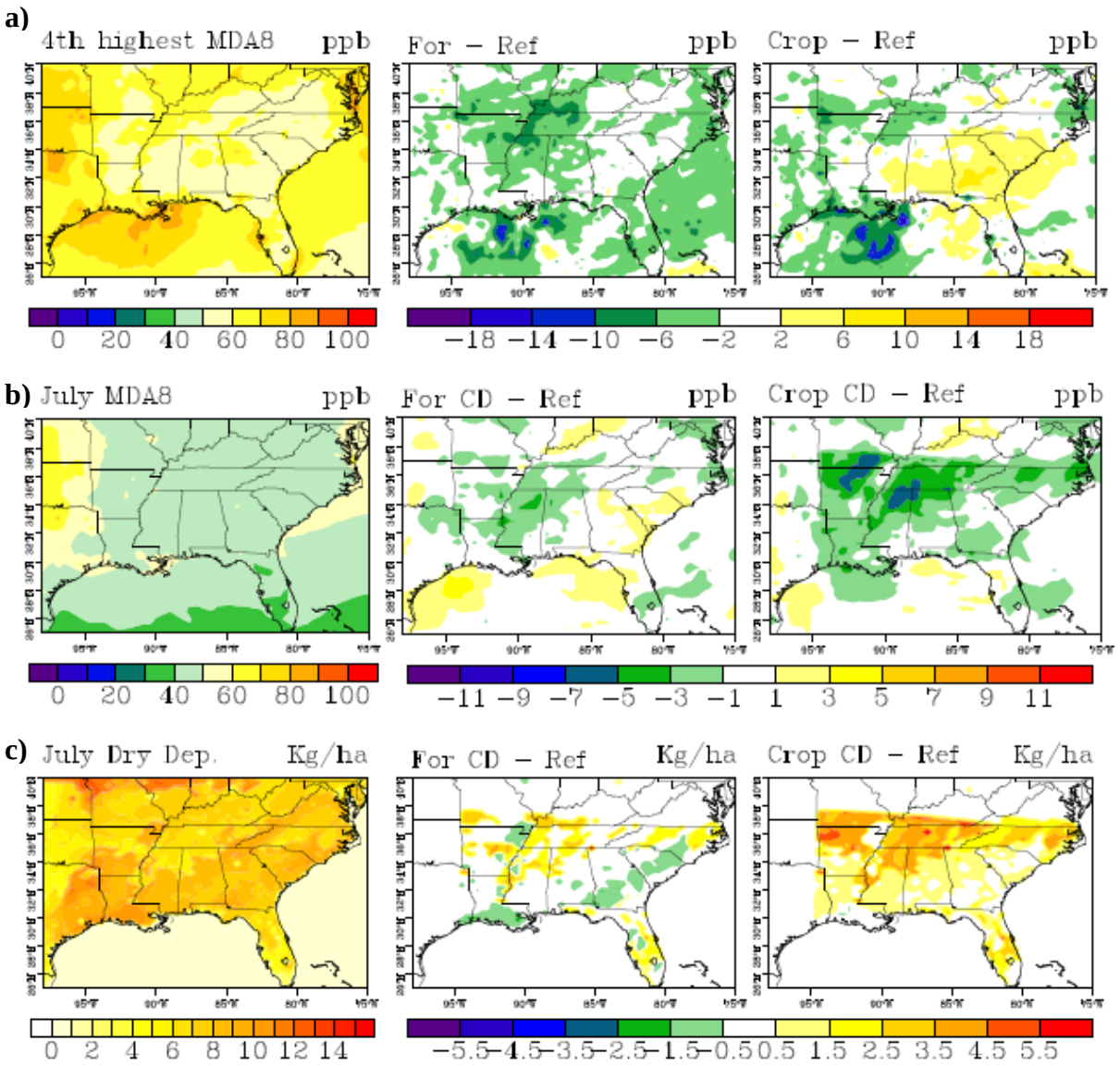

Figure 2 (a) 4th highest MDA8 mixing ratio of the year (left) and the difference (scenario minus reference case) in the 4th highest MDA8 for the reforestation scenario (middle) and the cropland conversion scenario (right). (Little change is found outside of the Southeast so we focus on that area) **(b)** MDA8 averaged over the month of July for the reference CD case (left) and the difference (scenario minus reference case) in the July average MDA8 for the reforestation scenario (middle) and the cropland conversion scenario (right). **(c)** The same as (b) but for the total deposition of O_3.

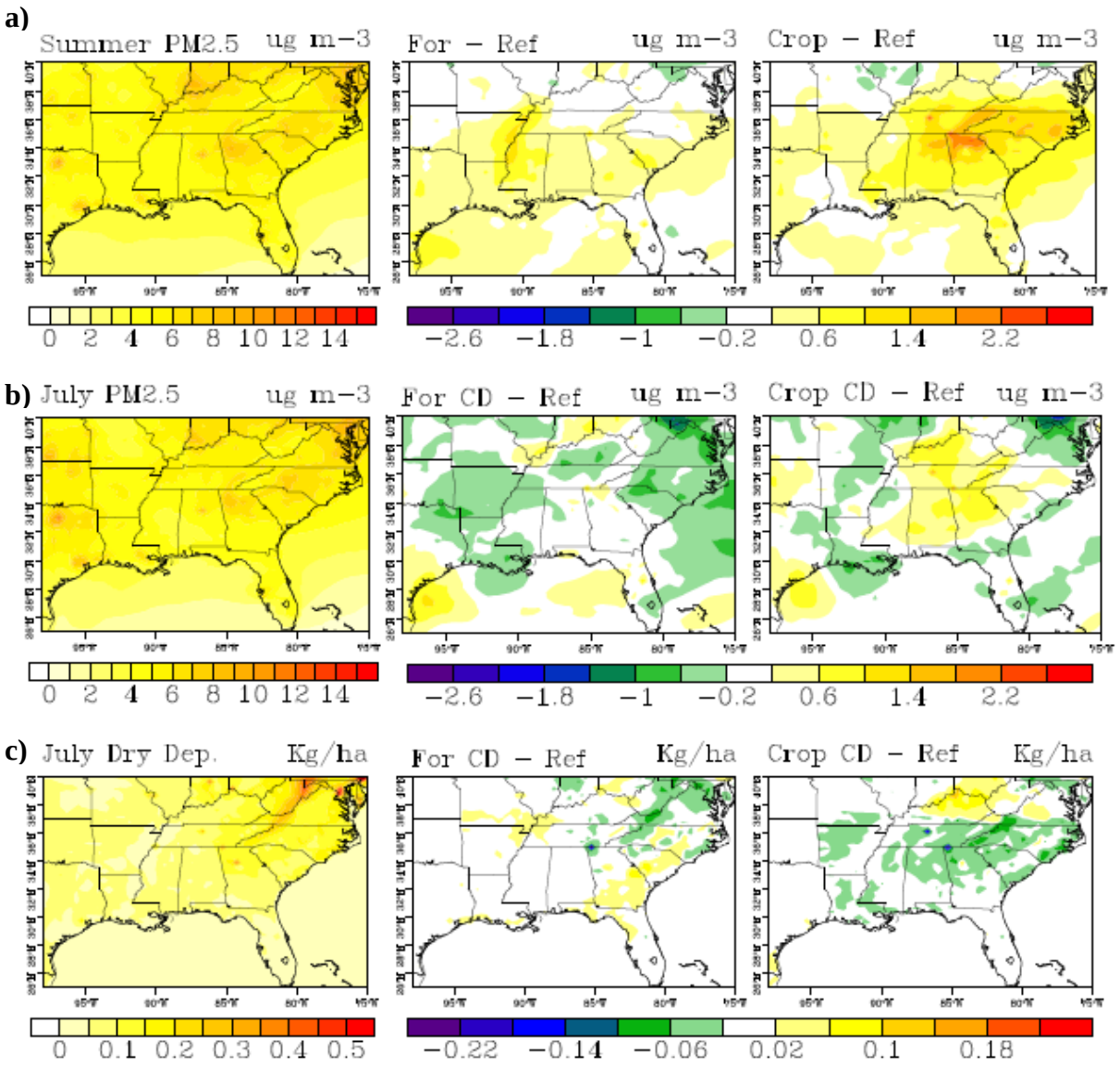

Figure 3 (a) Summertime (JJA) average $PM_{2.5}$ concentration for the reference case (left) and the difference (scenario minus reference case) in the summer time average $PM_{2.5}$ for the reforestation scenario (middle) and the cropland conversion scenario (right). (Little change is found outside of the Southeast so we focus on that area) **(b)** $PM_{2.5}$ averaged over the month of July for the reference CD case (left) and the difference (scenario minus reference case) in the July average $PM_{2.5}$ for the reforestation scenario (middle) and the cropland conversion scenario (right). **(c)** The same as (b) but for the total deposition of $PM_{2.5}$.

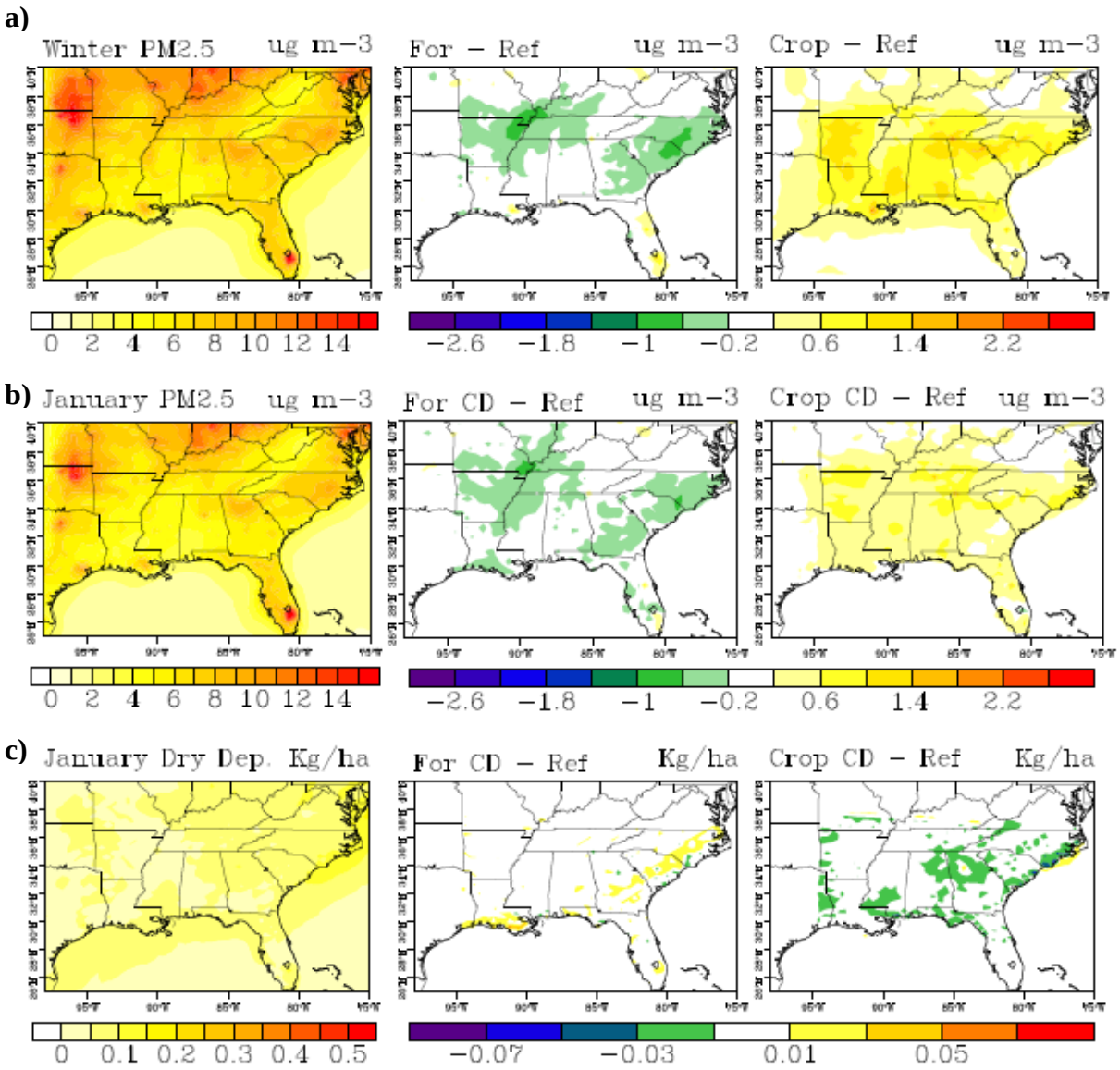

Figure 4 (a) Wintertime (DJF) average $PM_{2.5}$ concentration for the reference case (left) and the difference (scenario minus reference case) in the wintertime average $PM_{2.5}$ for the reforestation scenario (middle) and the cropland conversion scenario (right). (Little change is found outside of the Southeast so we focus on that area) **(b)** $PM_{2.5}$ averaged over the month of January for the reference CD case (left) and the difference (scenario minus reference case) in the January average $PM_{2.5}$ for the reforestation scenario (middle) and the cropland conversion scenario (right). **(c)** The same as (b) but for the total deposition of $PM_{2.5}$.